Pergamon

Bioorganic & Medicinal Chemistry 7 (1999) 2473–2485

BIOORGANIC & MEDICINAL CHEMISTRY

Molecular Recognition of Tyrosinyl Adenylate Analogues by Prokaryotic Tyrosyl tRNA Synthetases

Pamela Brown,* Christine M. Richardson,* Lucy M. Mensah, Peter J. O'Hanlon, Neal F. Osborne, Andrew J. Pope and Graham Walker

SmithKline Beecham Pharmaceuticals, New Frontiers Science Park, Third Avenue, Harlow, Essex, CM19 5AW, UK

Received 26 February 1999; accepted 4 June 1999

Abstract—Molecular modelling and synthetic studies have been carried out on tyrosinyl adenylate and analogues to probe the interactions seen in the active site of the X-ray crystal structure of tyrosyl tRNA synthetase from *Bacillus stearothermophilus*, and to search for new inhibitors of this enzyme. Micromolar and sub-micromolar inhibitors of tyrosyl tRNA synthetases from both *B. stearothermophilus* and *Staphylococcus aureus* have been synthesised. The importance of the adenine ring to the binding of tyrosinyl adenylate to the enzyme, and the importance of water-mediated hydrogen bonding interactions, have been highlighted. The inhibition data has been further supported by homology modelling with the *S. aureus* enzyme, and by ligand docking studies.

Introduction

Aminoacyl tRNA synthetase enzymes play a key role in protein biosynthesis. The enzymes are responsible for charging a tRNA molecule with its appropriate amino acid with extremely high fidelity. Any mistakes at this level lead to the mis-incorporation of amino acids into proteins.

We have shown that the selective inhibition of bacterial isoleucyl tRNA synthetase by pseudomonic acid and its synthetic analogues gives rise to potent antibacterial activity.[1] We sought to examine the inhibition of other synthetases as a source of new potential antibacterial agents. In this paper we describe the synthesis and molecular modelling of novel compounds to probe the molecular interactions seen in the active site of tyrosyl tRNA synthetase.

The tRNA synthetase enzymes act by a two-step mechanism. In the first stage, the enzyme recognises the appropriate amino acid and activates this by reaction with ATP to produce an aminoacyl adenylate; in this case, tyrosyl adenylate (Tyr-AMP) (**1**), which remains bound to the enzyme. In the second step, the enzyme catalyses the transfer of the amino acid onto its cognate tRNA (Scheme 1).

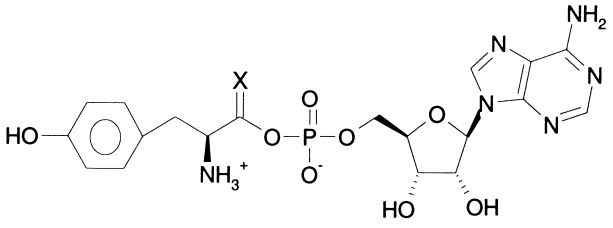

(**1**) X = O Tyrosyl adenylate

(**2**) X = H_2 Tyrosinyl adenylate

Crystallographic information is available on tyrosyl tRNA sythetase (YRS) from *Bacillus stearothermophilus* both in its native form and in a complex with the inhibitor, tyrosinyl adenylate (**2**) (Brookhaven codes 2ts1 and 3ts1).[2] A number of polar interactions can be observed in the 2.7 Å resolution *B. stearothermophilus* enzyme–ligand complex, which are shown in Figure 1. The importance of the key interactions with tyrosine has been noted elsewhere.[3] The aim of the present study was to investigate three specific areas of the adenylate interactions; the phosphate moiety, the role of the ribose hydroxyl groups, and the specificity of the adenine binding

E + Tyr + ATP ➡ E.Tyr-AMP + PPi ➡ E + AMP + Tyr-tRNA

Scheme 1.

Key words: Amino acids and derivatives; enzyme inhibitors; molecular modelling; X-ray crystal structures; homology modelling.

* Corresponding authors.

0968-0896/99/$ - see front matter
PII: S0968-0896(99)00192-3

region. Molecular modelling and synthetic studies were undertaken to investigate the relative importance of these interactions and to probe the active site for other factors important in molecular recognition. A homology model of tyrosyl tRNA synthetase from the pathogenic organism *Staphylococcus aureus* was also generated and the inhibitory effects of the analogues on the enzymes from both sources was determined.

Results

Chemistry

Aminoalkyl adenylates have been prepared by condensation of the appropriate amino alcohol with AMP.[4] However, the recently-described phosphoramidite coupling approach[5] appeared to provide the versatility required for the synthesis of structural variants. Our initial approach to the synthesis of tyrosinyl adenylate (**2**) was to activate the 5′ position of the protected adenosine (**3**) by reaction with diisopropyl phosphonamidic chloride. The resultant phosphoramidite was highly reactive, and was coupled directly with bis-CBZ-protected L-tyrosinol followed by iodine oxidation to give the protected phosphotriester (**4**) (Scheme 2). Treatment with *n*-butylamine to remove the N^6-benzoyl, methyl ester and O-CBZ groups, followed by hydrogenolysis of the amine protecting group gave the 2′,3′-*O*-isopropylidene derivative (**5**). This was deprotected with 40% aqueous TFA to give tyrosinyl adenylate (**2**). As a probe to the binding region around the adenine ring, the N^6-benzoyl group was retained by deprotection of the phosphomethyl ester with *t*-butylamine. Hydrogenolysis followed by removal of the isopropylidine group gave the derivative (**6**).

For a more general approach to tyrosinol-derived phosphodiesters, phosphoramidite activation of the tyrosinol moiety, followed by displacement by the 5′-hydroxy group of the nucleoside analogue appeared a more versatile strategy. Thus bis-CBZ tyrosinol was converted to the cyanoethyl phosphoramidite (**7**) which was stable to storage in the freezer under an argon atmosphere. Reaction of this with the appropriate protected nucleoside analogues followed by deprotection of the phosphotriester with methanolic ammonia gave, after further deprotection, the 2′-deoxy (**8**), 3′-deoxy (**9**) and uridine (**10**) analogues of tyrosinyl adenylate, as shown in Scheme 3.

The cyanoethyl phosphoramidite (**7**) proved insufficiently reactive in some cases however, and the corresponding methyl phosphoramidite was prepared and used in situ (Scheme 4). This route was used in the synthesis of analogues designed to probe the requirements around the adenine binding region, the unsubstituted ribose (**11**), naphthyl (**12**) and α,β-unsaturated ester (**13**). Also in this sequence, use of the *N*-Boc protected tyrosinol (**14**) afforded a simpler deprotection strategy.

Tyrosyl sulfamoyl adenosine (**15**) was synthesised by a procedure analogous to the reported methods[6–8] (Scheme 5). As a variant of this, the acyl sulfamide (**17**) was prepared from the 5′-amino adenosine (**18**) via the sulfamide (**19**) (Scheme 6).

Swern oxidation of the protected adenosine (**3**) gave the aldehyde (**20**) which could be reacted in situ with the Wittig reagent **21** derived from L-tyrosinol (Scheme 7), to give after deprotection, the (*E*)-α,β-unsaturated ester (**22**).

Modelling

Tyrosinyl adenylate (**2**) and analogues (**5**–**6**, **8**–**13**, **15**, **17** and **22**) were modelled in the active site of the *B. stearothermophilus* tyrosyl tRNA synthetase enzyme. This docking work was performed using the CHARMm force field and the resulting model complexes were visualised using Quanta.[9]

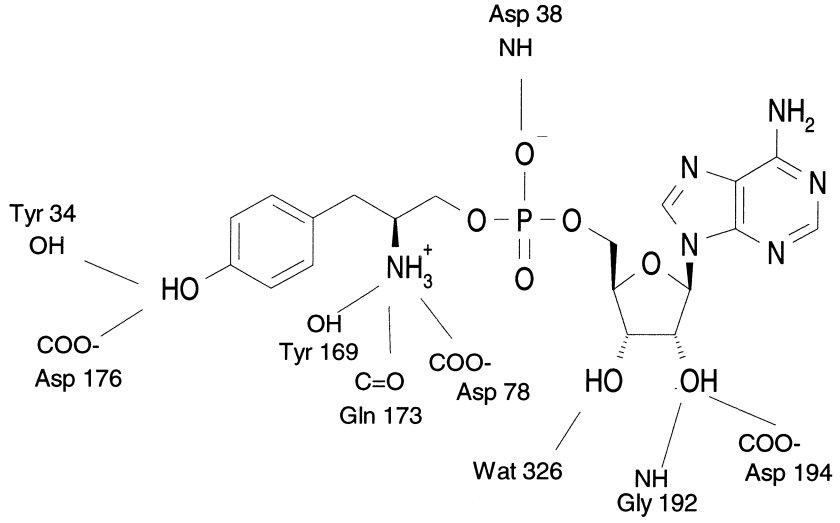

Figure 1. Polar interactions from tyrosinyl adenylate to residues in the active site taken from the X-ray structure.[2]

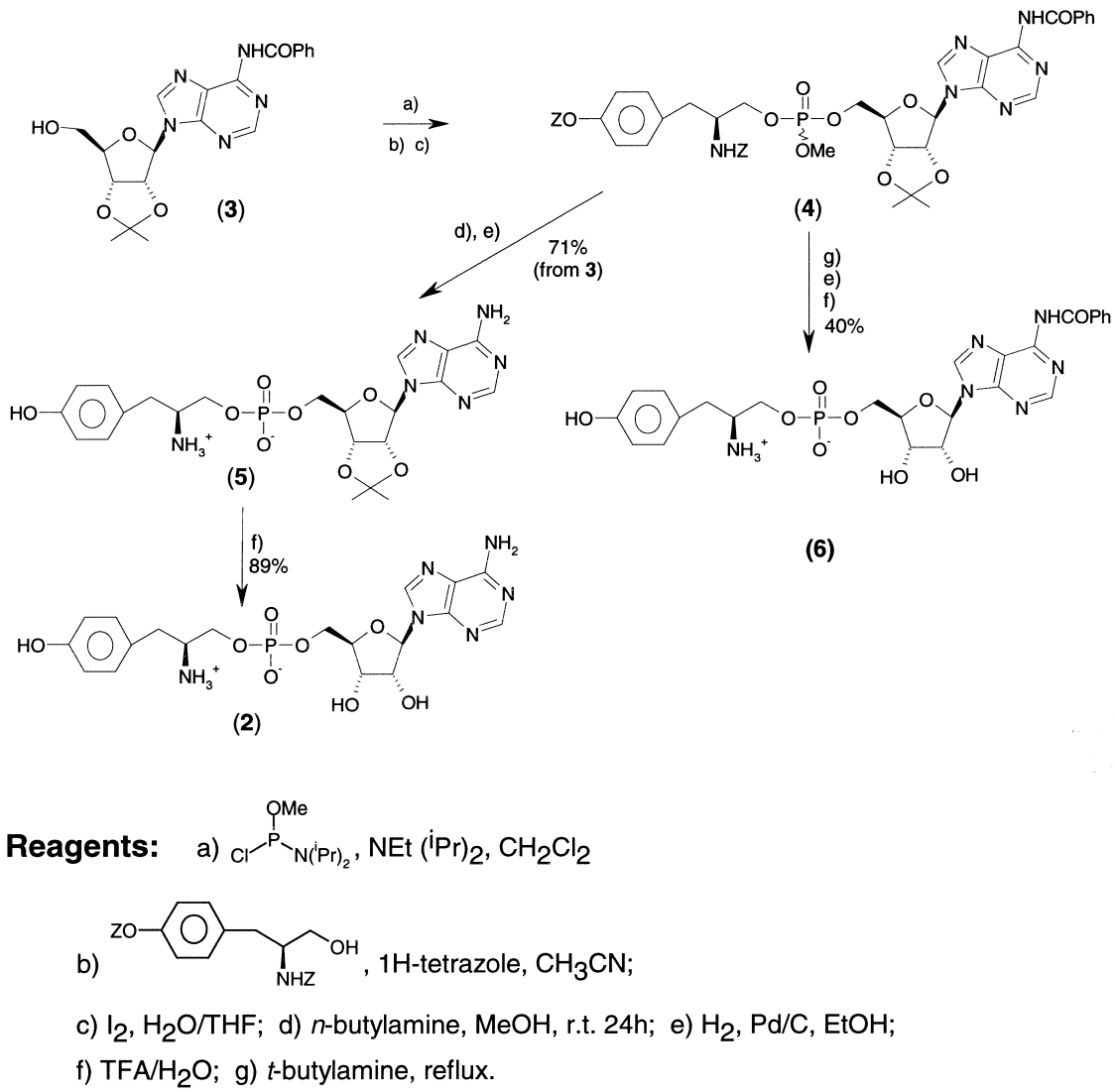

Scheme 2.

Phosphate replacements

The phosphate unit of tyrosinyl adenylate lies in a solvent exposed region of the active site (Fig. 2) and appears to make only one polar interaction directly with the protein.

Tyrosyl sulfamoyl adenosine (**15**) was of interest because sulfamates have been demonstrated to be potent inhibitors of the seryl, alanyl and prolyl tRNA synthetase enzymes,[6–8] all of which belong to a different structural class of tRNA synthetases from that of the tyrosyl studied here.[10,27] Molecular modelling showed this compound to fit well within the active site of the tyrosyl tRNA synthetase enzyme. Docking the sulfamide (**17**) showed evidence of some distortion of both protein and ligand. The α,β-unsaturated ester (**22**) is a significant departure from the phosphate unit of tyrosinyl adenylate in terms of both charge and rigidity. Compound (**22**) docked well in the active site, with minimal strain in the ligand and no significant deformation of the protein backbone around the active site.

Ribose modifications

The crystal structure of the tyrosinyl adenylate–tyrosyl tRNA synthetase complex shows that the 2′ ribose hydroxyl makes an interaction to the side chain of Asp 194 and also hydrogen bonds to the backbone NH of Gly 192. The 3′ ribose hydroxyl appears to interact with a highly ordered water molecule, which is itself embedded in an extended hydrogen bonding network. The 2′ and 3′ deoxyribose analogues (**8**) and (**9**) were modelled in the active site. 3′-Deoxyribose is known to adopt a different conformation to the 2′-deoxy analogue so these compounds were docked using the preferred deoxyribose conformations taken from the Cambridge Structural Database.[11] However, it was still possible to dock the 3′-deoxy variant (**9**) while maintaining the interaction between the 2′ sugar hydroxyl and the Asp194 side chain. The isopropylidene derivative of tyrosinyl adenylate (**5**) appeared too sterically demanding to bind in the active site in a consistent manner to tyrosinyl adenylate.

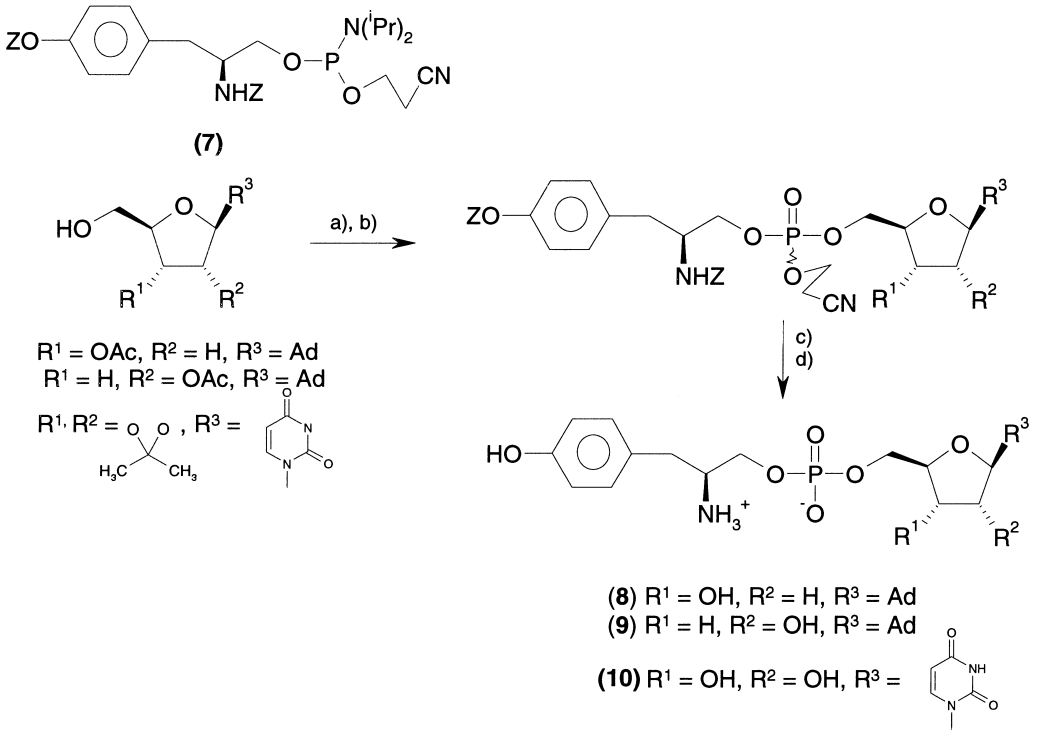

Reagents: a) (**7**), 1-H tetrazole, CH_3CN, b) I_2/H_2O/THF

c) NH_3, MeOH, d) H_2, Pd/C

Scheme 3.

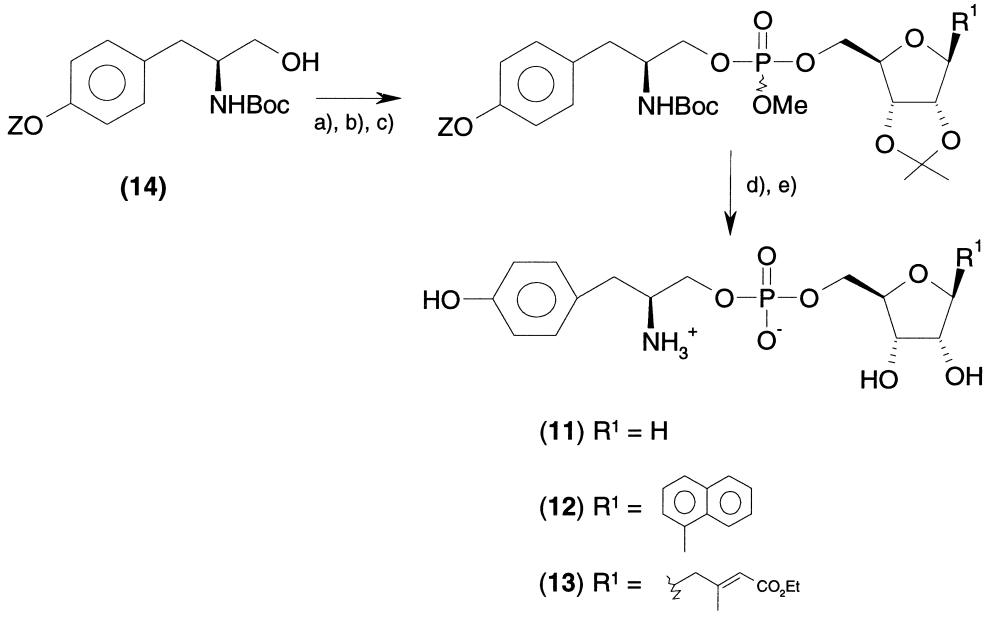

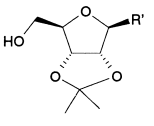

Reagents: a) 

, $NEt(^iPr)_2$, CH_2Cl_2; b) 1H-tetrazole, CH_3CN,

c) I_2, H_2O/THF; d), *n*-butylamine, MeOH; e) TFA/H_2O

Scheme 4.

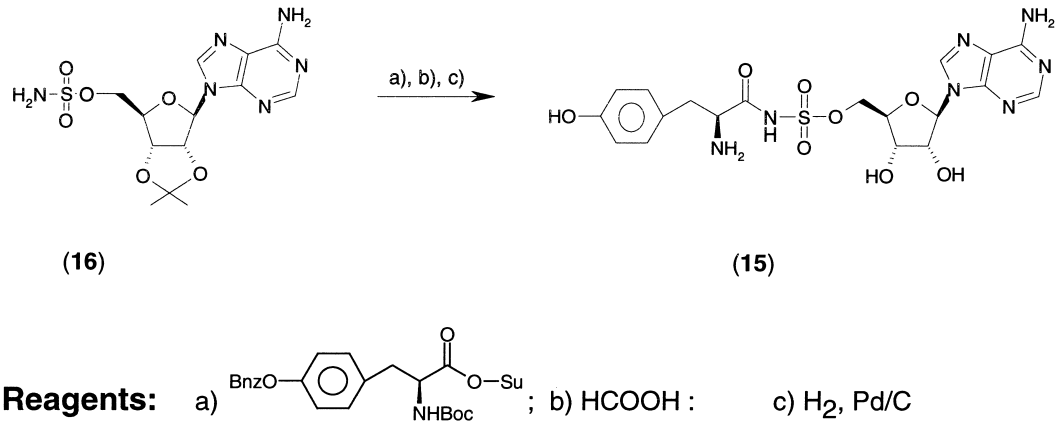

Scheme 5.

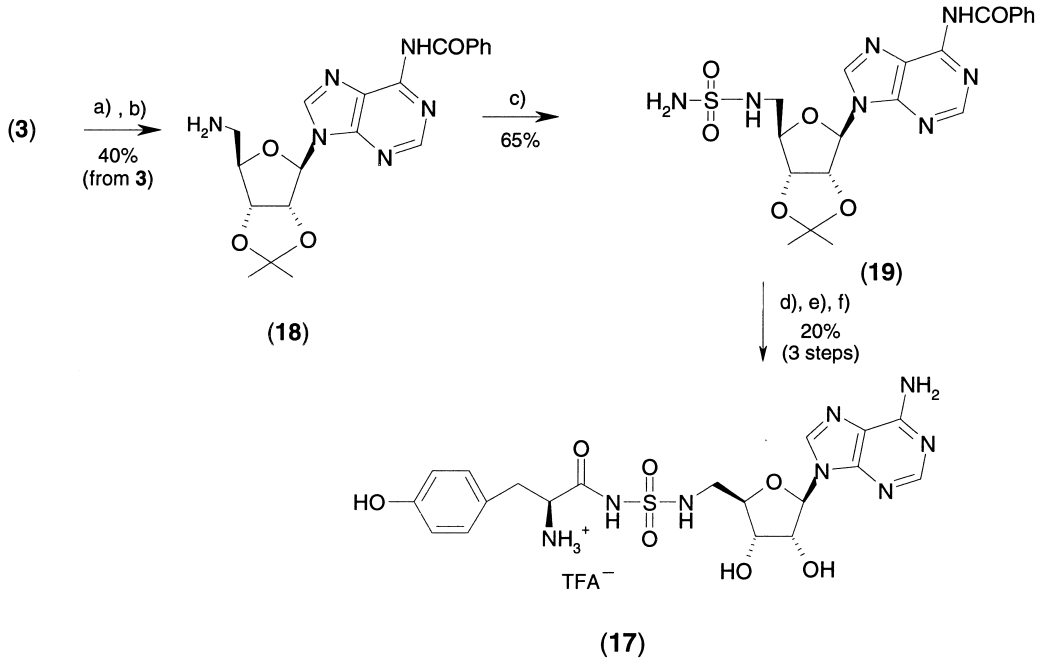

Scheme 6.

Probing adenine recognition

The adenine ring appears to make no significant polar interactions in the tyrosinyl adenylate complex. Modelling studies suggested that water mediated hydrogen bonds may be present but no highly ordered water molecules are observed in structural data on this region of the active site. The adenine binding pocket appeared large enough to accommodate the N^6-benzoyl group of (**6**). Modelling showed the unsubstituted compound (**11**) and the 1-naphthyl (**12**) to be well tolerated, with no significant movement within the protein backbone. The uracil analogue (**10**) docked well into the active site, although the ribose ring appeared in the flipped orientation compared to that in adenosine. Hydrogen bonding to the 2′ ribose hydroxyl was preserved and the uracil group moved out to interact with lysine 228, one of the lysines present in the mobile KMSKS loop. Compound (**13**) contains the α,β-unsaturated ester group similar to that found in mupirocin, a potent inhibitor of isoleucyl tRNA synthetase,[1] but can only be docked into the active site at the expense of some localised deformation of the protein backbone in the adenine binding pocket.

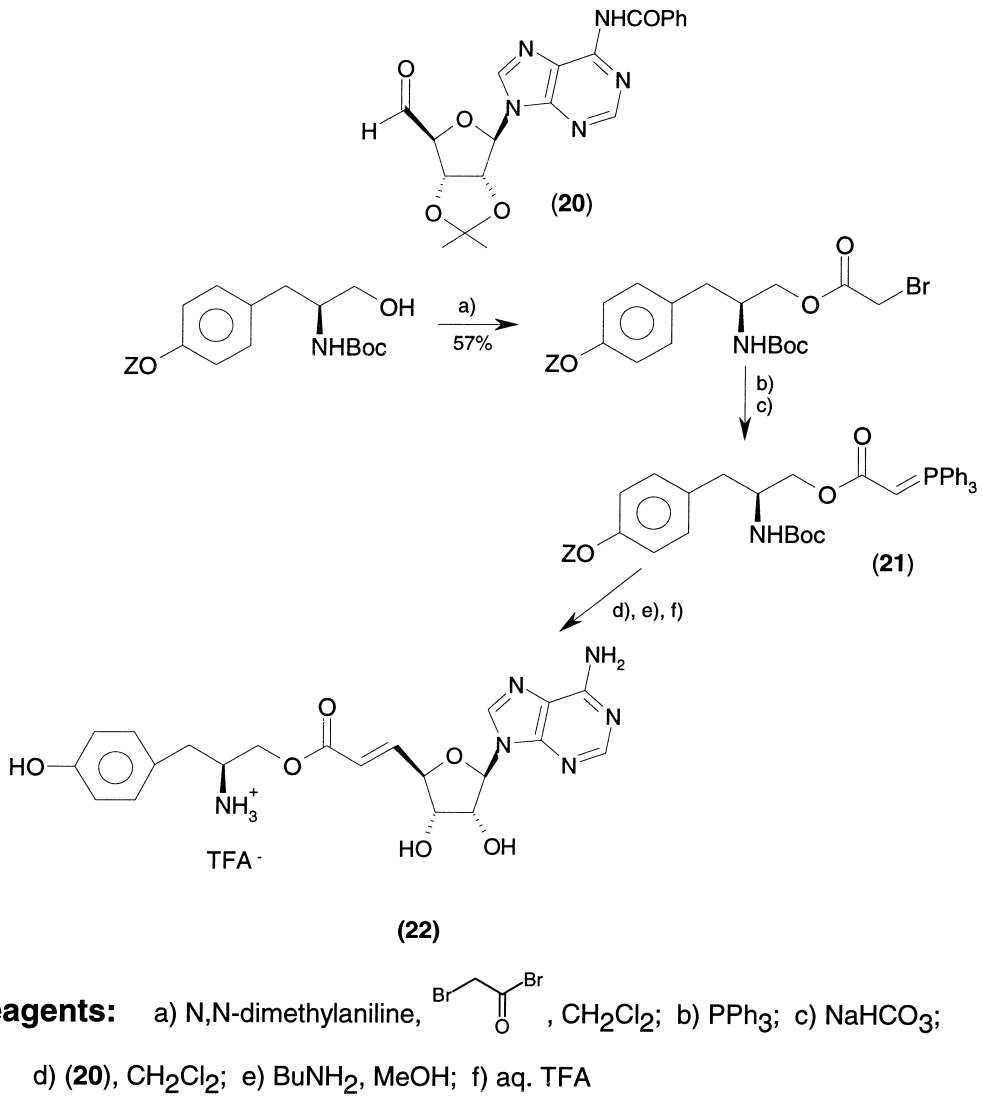

Scheme 7.

Homology modelling

The *S. aureus* tyrosyl tRNA synthetase sequence[12] shares 62% identity with that of the *B. stearothermophilus* (Fig. 3).

Homology modelling and ligand docking studies show no significant differences in either the shape of the active site or in the polar interactions that can be made between the enzyme and tyrosinyl adenylate in each case. From the alignment, and a comparison of residues which lie within 5 Å of the bound ligand in the *B. stearothermophilus* crystal structure, it can be seen that there are only three residues which differ between the *B. stearothermophilus* and *S. aureus* active sites. These are Phe37, Ala50 and Thr51, based on the *B. stearothermophilus* numbering. Phe37 is paired with Ile52 in the *Bacillus* enzyme and this corresponds to a match between Ala39 and Phe54 in the *Staphylococcus* enzyme. Therefore, the overall active site shape is very similar. Ala50 lies at the end of the adenine binding cleft and Thr51 is located above the ribose ring of tyrosinyl adenylate. Thr51 does not bind to tyrosinyl adenylate in the complex but is believed to stabilise the transition state for the aminoacylation reaction.[14]

Biochemical evaluation

Tyrosinyl adenylate (**2**) and analogues (**5**–**6**, **8**–**13**, **15**, **17** and **22**) were tested as inhibitors of YRS from 2 sources. The inhibition of YRS from *B. stearothermophilus* was determined by examining the effect on aminoacylation of $tRNA^{tyr}$ with ^{14}C-tyrosine. The inhibition of purified recombinant *S. aureus* enzyme was determined by a modified PPi/ATP exchange reaction. The results are given in Table 1.

Discussion

Tyrosinyl adenylate (**2**) was found to inhibit the *S. aureus* enzyme with an IC_{50} of 11 nM. This is in agreement with the level of inhibition reported against the *Escherichia coli* enzyme.[15]

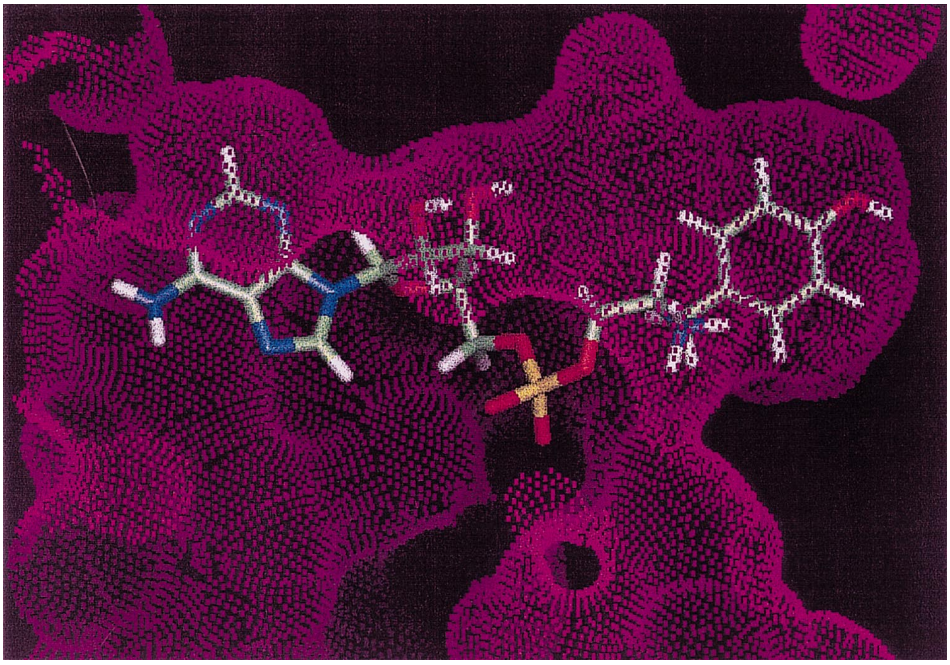

Figure 2. Tyrosinyl adenylate bound in the active site of the *Bacillus stearothermophilus* tyrosyl tRNA synthetase. A Connelly representation of the enzyme surface is shown by the purple dots. The tyrosine binding pocket and the adenine binding cleft are clearly visible.

Phosphate replacements

The sulfamate **15** was found to be an extremely potent inhibitor of both *Bacillus* and *Staphylococcus* enzymes. The compounds containing other phosphate replacements were poor. The modelling would suggest that this results from a combination of increased rigidity and unfavourable steric interactions in the case of the sulfamide (**17**). The α,β-unsaturated ester linkage of compound (**22**) cannot make the polar interaction observed between the phosphate of tyrosinyl adenylate and the backbone NH of Asp38.

Ribose analogues

Protection of the ribose moiety with an isopropylidene derivative produced an inactive compound (**5**), in good agreement with the docking studies. The two deoxyribose variants also showed a loss in activity. The 2′-deoxyribose (**8**) showed a 30-fold reduction in enzyme inhibition, which correlates well with the loss of a hydrogen bond between a hydroxyl group and a charged residue.[14] The 60-fold reduction in activity caused by removal of the 3′ hydroxyl group from tyrosinyl adenylate was greater than expected from interaction of this hydroxyl with a neutral NH group and a water molecule. However, this water molecule has a very low temperature factor and forms part of an extended hydration network in the X-ray structure (PDB code 3ts1). The 3′ hydroxyl of tyrosinyl adenylate replaces a second highly ordered water which is found in the structure of YRS with no ligand (PDB code 2ts1) and forms part of this network. Displacing this tightly bound water molecule without compensating for the loss of its enthalpic interaction with the protein may be energetically unfavourable, despite the corresponding increase in the entropy contribution to the free energy of the system.

Adenine variants

Removal of the adenine moiety of tyrosinyl adenylate in (**11**) had a substantial impact, confirming that recognition of the adenine ring is significant for inhibitor binding. The naphthyl variant (**12**) shows improved activity over the unsubstituted compound, but is still considerably poorer than tyrosinyl adenylate (**2**). This suggests that polar interactions in this region are substantially more important than is initially apparent from the structural data. The uridine (**10**) has good activity and this may be consistent with the polar interactions seen in the docking model. The α,β-unsaturated ester **13** showed very poor activity. This is consistent with the backbone movement observed in the docking model and shows that this fragment is not a suitable adenine replacement within this chemical series.

Conclusions

We have synthesised a variety of inhibitors of tyrosyl tRNA synthetase with alterations in the adenine, ribose and phosphate regions of tyrosinyl adenylate. While we have found that the level of inhibition of tyrosinyl adenylate can be maintained by replacement of the phosphate with the sulfamate moiety, other variants led to substantially decreased potency. Homology modelling studies have shown that the *S. aureus* and *B. stearothermophilus* enzymes are very closely related, supporting the similar trends seen in the inhibition of the

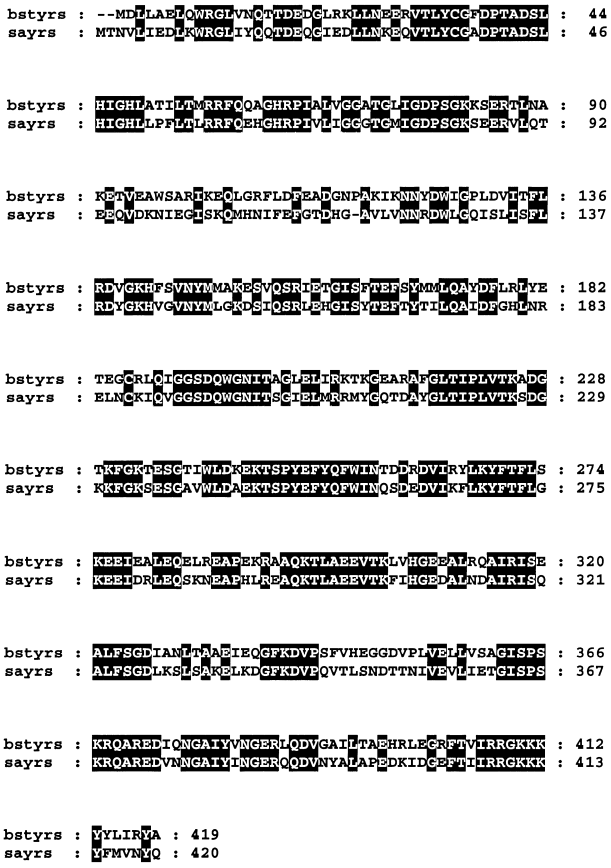

Figure 3. Alignment of the sequences of the *Bacillus stearothermophilus* tyrosyl tRNA synthetase enzyme and the *S. aureus* tyrosyl tRNA synthetase enzyme. The alignment is displayed using Genedoc.[13]

Table 1. Inhibition of tyrosyl tRNA synthetase (IC_{50} (μM))

		Staphylacoccus aureus	*Bacillus stearothermophilus*
Tyrosinyl adenylate	**2**	0.011	0.0063
Phosphate replacement	**5**	0.026	0.0093
	17	0% at 100 μM	NT[a]
	22	0% at 100 μM	NT
Ribose variants	**5**	NT	25% at 100 μM
	8	100	18
	9	140	36
Adenine variants	**6**	NT	0.68
	10	0.21	NT
	11	420	76
	12	150	5.7
	13	0% at 100 μM	NT

[a] NT, not tested.

two enzymes. In general, the modelling results are in good agreement with the biological data, although polar interactions do appear to be more important in adenine recognition than immediately apparent from the crystallographic data. This is at least in part due to limitations imposed by the crystal structure resolution. The study has also highlighted the importance of the highly ordered water molecules which are present in the crystallographic data and which assist in defining the polar interactions in the active site.

Experimental

Chemistry

Infrared spectra were determined either in dichloromethane on a Philips PU 9706 spectrophotometer, or in KBr on a Perkin–Elmer PE 983 spectrophotometer. NMR spectra were recorded on a Bruker AC-250F spectrometer. Chemical shifts are expressed in ppm (δ) relative to internal tetramethylsilane. Mass spectra were obtained on a VG ZAB mass spectrometer.

All organic phases were dried over anhydrous $MgSO_4$, and the solvent removed under reduced pressure with a Büchi rotary evaporator. Merck Kieselgel 60 (< 230 mesh ASTM) was used for column chromatography of intermediates. Tetrahydrofuran (THF) was dried by distillation from calcium hydride followed by distillation from sodium benzophenone ketyl.

Target compounds were purified on Mitsubishi Diaion HP20SS, and the purity was confirmed by HPLC. HPLC was performed on a Waters Associates instrument using a C_{18} μ-Bondapak reverse-phase column with pH 4.5 0.05 M ammonium acetate buffer-methanol solutions as eluant. Detection was by UV at 240 nm and at the λ_{max} of the test compound.

L-Tyrosinyl-2′,3′-*O*-isopropylidene adenylate (5). N^6-Benzoyl adenosine[16] (820 mg, 2.0 mmol), was dissolved in acid-free dichloromethane (8 mL), containing diisopropylethylamine (1.3 mL, 6.66 mmol). To this was added *N,N*-diisopropylmethyl phosphonamidic chloride (0.58 mL, 3.0 mmol) at room temperature under an argon atmosphere. After 15 min, the solution was transferred with 100 mL ethyl acetate (pre-washed with saturated $NaHCO_3$) into a separating funnel and washed with saturated $NaHCO_3$. The organic phase was dried ($MgSO_4$), and evaporated. The crude product was dissolved in dry acetonitrile and treated with *N,O*-bis benzyloxycarbonyl tyrosinol, followed by 1 H-tetrazole (0.871 g, 10 mmol) at room temperature under an argon atmosphere. After 15 min, the solution was treated with a solution of iodine (490 mg, 2.0 mmol) in 1:1 THF: water (100 mL) together with 2,6-lutidine (2.3 mL, 20 mmol). After 15 min, the solution was diluted with ethyl acetate (200 mL), washed with 5% aqueous sodium bisulfate, 5% citric acid, water and brine, dried ($MgSO_4$), and evaporated. The residue was chromatographed on Kieselgel 60 eluting with 0–5% methanol in CH_2Cl_2, to give the protected phosphodiester **4** as a white foam (0.723 g, 40%), as a 1:1 mixture of diasteromers at the phosphorus centre; δ_P ($CDCl_3$) 14.68, 14.72. *m/z* (ESI) 923 (MH^+, 100%). This material (380 mg, 0.41 mmol), was dissolved in methanol (10 mL) and *n*-butylamine (10 mL), and the reaction stirred at room temperature for 24 h. The solvent was evaporated and the residue chromatographed on Kieselgel 60 eluting with 20–40% methanol in CH_2Cl_2, to give the N^6-deprotected compound as a white foam (220 mg, 81%). 180 mg of this material (0.27 mmol) was dissolved in 50% aqueous dioxan (30 mL), acetic acid (0.15 mL) added followed by 10% Pd/C, and the mixture hydrogenated at room temperature and pressure for 1.5 h.

The mixture was filtered, concentrated under reduced pressure, and the pH adjusted to 7 with saturated $NaHCO_3$ and the aqueous phase chromatographed on HP20SS eluting with 0–20% THF in water. Product-containing fractions were freeze-dried to give **5** as a white solid (60 mg, 41%); υ_{max} (KBr) 3353, 1647 and 1602 cm^{-1}; λ_{max} (H_2O) 260 nm (ε_m 12,322); δ_H (D_2O) 1.45 (3H, s, CH_3), 1.63 (3H, S, CH_3), 2.55 (2H, ABx, $J=7.0$, 14.1, 32.5 Hz), 3.38–3.45 (1H, m), 3.55–3.79 (2H, m, OCH_2), 4.00–4.05 (2H, m, OCH_2), 4.55–4.60 (1H, m), 5.10 (1H, dd, $J=2.62$, 6.22 Hz), 5.25 (lH, dd, $J=3.0$, 6.22 Hz), 6.18 (1H, d, $J=3.0$ Hz, 1′-H), 6.56 and 6.85 (4H, ABq, $J=8.5$ Hz, Ar-H), 8.10 (1H, s), 8.21 (1H, s); α_D^{25} −13° (c1, H_2O); *m/z* (ESI) 537 (MH^+, 100%).

L-Tyrosinyl adenylate (2). Compound **5** (40 mg, 0.075 mmol) was dissolved in 40% aqueous TFA (2 mL) and stirred at room temperature for 4 h. The solvent was evaporated and the residue chromatographed on a column of HP20SS eluting with 2% THF/water. Product-containing fractions were freeze-dried to give **2** as a white solid (33 mg, 89%); υ_{max} (KBr) 3354, 1647 and 1610 cm^{-1}; λ_{max} (H_2O) 261 nm (ε_m 11,902), δ_H (D_2O) 2.60 (2H, ABx, $J=7.0$, 14.8, 34.0 Hz), 3.50–3.57 (1H, m), 3.72–3.81 (2H, m, OCH_2), 4.08–4.15 (2H, m, OCH_2), 4.28–4.33 (1H, m), 4.40 (1H, t, $J=5.2$ Hz), 4.65 (1H, t, $J=4.5$ Hz), 6.01 (1H, d, $J=4.3$ Hz, 1′-H), 6.56 and 6.86 (4H, ABq, $J=7.9$ Hz, Ar-H), 8.16 (1H, s), 8.28 (1H, s); *m/z* (ESI) 497 (MH^+, 100%).

L-Tyrosinyl N^6-benzoyl adenylate (6). Compound **4** (100 mg, 0.108 mmol) was dissolved in *t*-butylamine (7 mL) and heated to reflux for 6 h. The mixture was evaporated under reduced pressure to a white foam. This was dissolved in ethanol (10 mL), 10% Pd/C (50 mg) added and the mixture hydrogenated at room temperature and pressure. After 3 h, a further 50 mg of catalyst was added and hydrogenation continued for a further 2 h. The mixture was filtered through Kieselguhr, the catalyst washed with water, and the filtrated evaporated to dryness. The residue was chromatographed on Kieselgel 60 eluting with 20–50% methanol in CH_2Cl_2, to give the isopropylidene compound as a white foam (40 mg, 58%). This was dissolved in 40% aqueous TFA (4 mL) and stirred at room temperature for 4 h. The solvent was evaporated and the residue chromatographed on a column of HP20SS eluting with 2–10% THF/water. Product containing fractions were freeze-dried to give **6** as a white solid (15 mg, 40%); υ_{max} (KBr) 3336, 1702 and 1615 cm^{-1}; λ_{max} (H_2O) 281 nm (ε_m 16,929), δ_H (D_2O) 2.50 (2H, ABx, $J=7.3$, 14.2, 33.1 Hz), 3.47–3.53 (1H, m), 3.72–3.91 (2H, m, OCH_2), 4.08–4.17 (2H, m, OCH_2), 4.32–4.38 (1H, m), 4.49 (1H, t, $J=5.2$ Hz), 4.76 (1H, t, $J=4.8$ Hz), 6.16 (1H, d, $J=4.2$ Hz, 1′-H), 6.50 and 6.82 (4H, ABq, $J=8.4$ Hz, Ar-H), 7.50–7.72 (3H, m, Ar-H), 7.90–7.95 (2H, m, Ar-H), 8.5 (1H, s), 8.68 (1H, s); $\alpha_D^{25}=-4°$ (c1, H_2O); *m/z* (ESI) 601 (MH^+, 100%).

L-Tyrosinyl 2′-deoxy adenylate (8). To a solution of bis-CBZ tyrosinol (1.0 g, 2.2 mmol) in acid-free dichloromethane (8 mL), was added *N*-ethyl-*N,N*-diisopropylamine (1.4 mL, 3.3 mmol) followed by 2-cyanoethyl *N,N*-diisopropylphosphoramidite (0.73 mL, 3.3 mmol), and the mixture stirred at room temperature under argon for 20 min. The solution was diluted with ethyl acetate (50 mL), washed with saturated $NaHCO_3$ and brine, dried over anhydrous Na_2SO_4 and evaporated to **7**; *m/z* (NH_3 + DCI) 636 (MH^+, 2%).

A solution of **7** (1.4 g, 2.2 mmol), in dry acetonitrile (10 mL) was treated with 1 H tetrazole (154 mg, 2.2 mmol) followed by 3′-*O*-acetyl-*N*-benzoyl-2′-deoxyadenosine (100 mg, 0.25 mmol) in dry acetonitrile (3 mL). After 5 min dichloromethane (5 mL) was added followed after a further 5 min by 50 mg 1 H tetrazole. After stirring at room temperature for a further 20 min, the mixture was oxidised with iodine as described in the preparation of **2**. After work up, the crude product was dissolved in saturated methanolic ammonia (15 mL), and the solution stirred at room temperature for 20 h. The solvent was evaporated and the residue chromatographed on Kieselgel 60 eluting with 10–50% methanol in dichloromethane to give the protected intermediate as a white foam (151 mg, 98%); δ_H ($CDCl_3$) 2.27–2.53 (2H, m, CH_2), 2.55–2.63 (2H, m, CH_2), 4.85 (2H, ABq, $J=12.5$, 10.8 Hz, CH_2Ar), 6.28 (1H, t, $J=6.21$ Hz), 6.52 and 6.85 (4H, ABq, Ar-H), 7.08–7.15 (5H, m, Ar-H), 8.08 (1H, s), 8.25 (1H, s).

This material (145 mg, 0.24 mmol) was hydrogenated as described in the preparation of **5**. After chromatography and freeze-drying, **8** was obtained as a white solid (82 mg, 73%); λ_{max} (KBr) 3402, 1652 and 1606 cm^{-1}; λ_{max} (H_2O) 260 nm (ε_m 10,795), δ_H (D_2O) 2.43 (2H, Abq, $J=13.4$, 22.3 Hz), 2.58–2.78 (2H, m, 2′H_2), 3.14–3.18 (1H, m, 2″H), 3.53–3.71 (2H, m, 1″H_2), 4.08 (2H, br s, 2′H_2), 4.64–4.68 (1H, m, 3′-H), 6.45 (1H, t, $J=6.5$ Hz, 1′H), 6.62 and 6.86 (4H, ABq, $J=8.4$ Hz, Ar-H), 8.20 (1H, s), 8.32 (1H, s); *m/z* (ESI) 481 ($MH+$, 70%), 503 (MNa^+, 100).

L-Tyrosinyl 3′-deoxy adenylate (9). Protected 2′-*O*-acetyl-N^6-benzoyl-3′-deoxy adenosine (50 mg, 0.125 mmol) was coupled with **7**, followed by iodine oxidation and work up as described in the preparation of **2**. Treatment of the crude product with methanolic ammonia as previously described followed by column chromatography afforded the CBZ-protected product in 64% yield. This was hydrogenated as described for **5** followed by TFA deprotection. Chromatography on HP20SS gave **9** as a white freeze-dried solid (24 mg, 77%); υ_{max} (KBr) 3386, 1642, and 1609 cm^{-1}; λ_{max} (H_2O) 261 nm (ε_m 10,794), δ_H (d_6-DMSO) 1.91–1.97 and 2.23–2.28 (2H, m, 3′H_2) 2.50 (2H, ddd, $J=6.8$, 13.5, 53.8 Hz, 3″H), 3.01–3.04 (1H, m, 2″H), 3.45–3.61 (2H, m, 1″-H), 3.75–3.89 (2H, m, 5′H_2), 4.41–4.45 (1H, m, 4′H), 4.55–4.58 (1H, m, 2′H), 5.70 (1H, br s, OH), 5.90 (1H, d, $J=2.3$ Hz, 1′H), 6.67 and 6.98 (4H, ABq, $J=8.4$ Hz), 7.23 (2H, br s, NH), 8.15 (1H, s), 8.42 (1H, s), 9.27 (1H, br s, OH); *m/z* (ESI) 481 (MH^+, 100%).

L-Tyrosinyl uridine-5′-*O*-phosphate (10). 2′,3′-Isopropylidineuridine (71 mg, 0.25 mmol) was coupled to **7** (0.58 g, 1.0 mmol) followed by iodine oxidation, and deprotection

with methanolic ammonia as described for **8**. The crude product was deprotected with 40% aqueous TFA as described in the preparation of **2** followed by hydrogenation to give **10** as a white solid after chromatography on HP20SS and freeze-drying (35 mg, 30%); υ_{max} (KBr) 3417, 3185, 2924, 1698 and 1684 cm^{-1}; λ_{max} (H_2O) 262 nm (ε_m 7,710), δ_H (D_2O) 2.93 (1H, dd, J = 9.2, 14.0 Hz, CH_2Ar), 3.05 (1H, dd, J = 6.4, 14.0 Hz, CH_2Ar), 3.78–3.83 (1H, m), 3.90–3.96 (1H, m), 4.01–4.08 (1H, m), 4.09–4.14 (1H, m, 4′-H), 4.19–4.23 (1H, m, 5′-H), 4.24–4.26 (1H, m, 3′-H), 4.27–4.29 (1H, m, 5′H), 4.32 (1H, t, J = 4.6 Hz, 2′H), 5.80 (1H, d, J = 8.1 Hz), 5.90 (1H, d, J = 3.6 Hz, 1′-H), 6.87 and 7.21 (4H, ABq, J = 8.4 Hz), 7.78 (1H, d, J = 8.1 Hz), m/z (ESI) 474 (MH^+, 100%).

L-Tyrosinyl 1,4-anhydro-D-ribitol-5-*O*-phosphate (11). To a solution containing *N*-Boc-L-(OZ)tyrosinol **14** (350 mg, 0.9 mmol), triethylamine (1.1 mL, 8.1 mmol) and dichloromethane (5 mL) at 0°C was added *N,N*-diisopropylmethyl phosphonamidic chloride (0.18 mL, 0.9 mmol). After 1 h at room temperature the solution was evaporated and the residue dissolved in a mixture of acetonitrile (5 mL) and dichloromethane (5 mL). A solution of 1,4-anhydro-2,3-*O*-isopropylidene-D-ribitol[18] (50 mg, 0.3 mmol) in dichloromethane (1 mL) was then added followed by tetrazole (320 mg, 3.6 mmol), and after 3 h at room temperature by a solution containing iodine (230 mg, 0.9 mmol), 2,6-lutidine (1.0 mL, 9.0 mmol), THF (5 mL) and water (5 mL). After a further 15 min the solution was diluted with ethyl acetate and washed successively with 5% aqueous sodium sulfite, 5% aqueous citric acid and brine, dried, evaporated, and chromatographed using methanol–dichloromethane mixtures to give the fully protected product as an oil consisting of a 1:1 mixture of diastereomers at phosphorus (110 mg, 56%). δ_H ($CDCl_3$) 1.45 (9H, s, *t*Bu), 1.31 and 1.68 (6H, 2s, CMe_2), 2.8–3.0 (2H, m, 3-H_2), 3.8 (3H, 2d, J = 7 Hz, OMe), 3.9–5.1 (10H, m), 5.22 (2H, s, ZCH_2), 7.1 and 7.3 (4H, ABq, tyrosyl aromatics), 7.4–7.5 (5H, m, benzyl); m/z (DCI) 652 (MH^+). This material was deprotected using the following sequence; the benzyloxycarbonyl group was first removed by treatment with *t*-butylamine (2 mL) and methanol (2 mL) overnight at room temperature followed by evaporation. The methyl ester was then removed by treating the resulting oil with *n*-butylamine (2 mL) and methanol (2 mL) for 3 days at room temperature and evaporation. Finally the Boc and acetonide groups were removed from this second product by treatment with trifluoroacetic acid (2 mL) and water (3 mL) for 3 h at room temperature, followed by evaporation and chromatography using HP20SS eluting with acetone–water mixtures to give **11** as its trifluoroacetate salt after freeze-drying (13 mg, 52%). υ_{max} (KBr) 1680 cm^{-1}; λ_{max} (H_2O) 274 nm (ε_m 5,948); δ_H (D_2O) 2.91 (2H, d, J = 8 Hz, 3-H_2), 3.6–4.0 (10H, m), 6.9 and 7.2 (4H, ABq, aromatics); m/z (DCI) 364 (MH^+).

L-Tyrosinyl 1-β-naphthyl-1,4-anhydro-D-ribitol-5-*O*-phosphate (12). A mixture containing 1-β-D-ribofuranosyl naphthalene[19] (520 mg, 2 mmol), *p*-toluenesulfonic acid (34 mg, 0.2 mmol), and acetone (10 mL) was stirred at room temperature for 2 h and then silver oxide (90 mg, 0.4 mmol) was added. The mixture was stirred at room temperature for a further 1 h and then filtered, dried ($MgSO_4$), evaporated and chromatographed using methanol–dichloromethane mixtures to give the acetonide as an oil (400 mg, 67%). δ_H ($CDCl_3$) 1.31 and 1.72 (6H, 2s, Me_2), 3.8–4.1 (2H, m, 5′-H_2), 4.2–4.3 (1H, m, 4′-H), 4.7–4.9 (2H, m, 2′-H and 3′-H), 5.62 (I H, d, J = 10.2 Hz, 1′-H), 7.5–8.2 (7H, m, aromatics). This material (180 mg, 0.6 mmol) was converted to the title compound as described in the preparation of **11** giving a **12** as a white powder (70 mg, 19%). υ_{max} (KBr) 1515 cm^{-1}; λ_{max} (H_2O) 282 nm (ε_m 8,532); δ_H (D_2O) 2.5–2.8 (2H, m, 3-H_2), 3.4–4.0 (9H, m), 6.6 and 6.9 (4H, ABq, tyrosyl aromatics), 7.4–8.2 (7H, m, naphthyl aromatics); m/z (ESI^+) 490 (MH^+).

L-Tyrosinyl 1-β-(*E*)-(3-ethoxycarbonyl-2-methylprop-2-enyl)-1,4-anhydro-D-ribitol-5-*O*-phosphate (13). A mixture of 5-*O*-*t*-butyldimethylsilyl-2,3-*O*-isopropylidene-β-D-ribofuranose[20] (3.6 g, 12 mmol), acetylmethylenetriphenylphosphorane (4.2 g, 13 mmol) and acetonitrile (60 mL) was heated at reflux overnight then evaporated and chromatographed using hexane–ethyl acetate mixtures to give 1-(5-*O*-*t*-butyldimethylsilyl - 2,3 - *O* - isopropylidene-β-D-ribofuranosyl)-2-propanone as an oil (2.8 g, 68%); δ_H ($CDCl_3$) 0.08 (6H, s, $SiMe_2$), 0.91 (9H, s, *t*Bu), 1.34, 1.53 and 1.57 (9H, 3s, 3×Me), 2.7–2.9 (2H, m, 1-H_2), 3.6–3.7 (3H, m, 4′-H and 5′-H_2), 4.1, 4.3 and 4.7 (3H, 3m, 1′-H, 2′-H and 3′-H).

To triethyl phosphonoacetate (4.4 g, 20 mmol) in THF (50 mL) at 0°C were added sodium hydride (800 mg, 60% in oil, 20 mmol), and, when the solution had become clear, the above ketone (1.7 g, 5 mmol) in THF (10 mL). After 60 h at room temperature, aqueous ammonium chloride–ethyl acetate partition and chromatography using hexane–ethyl acetate mixtures gave the TBDMS ether of the title compound as an inseparable mixture of isomers (1.5 g, 3.6 mmol, 72%). This mixture was deprotected by dissolving in THF (10 mL) and adding a solution of tetrabutylammonium fluoride in THF (5 mL, 1 M, 5.0 mmol). After 1 h at room temperature, aqueous ammonium chloride–ethyl acetate partition followed by careful chromatography using hexane–ethyl acetate mixtures gave ethyl (*E*)-4-(2,3-*O*-isopropylidene-β-D-ribofuranosyl)-3-methylbut-2-enoate as an oil (430 mg, 40%). The stereochemistry of this compound was determined by comparison with previously reported analogues.[21] δ_H ($CDCl_3$) 1.28 (2H, t, J = 7 Hz, ethyl), 1.35 and 1.68 (6H, 2s, CMe_2), 2.24 (3H, s, CMe), 2.54 (1H, d, J = 6 Hz, H-4), 3.63 (2H, m, 5-H_2), 4.1–4.2 (4H, m, 1′-H, 4′-H, and ethyl), 4.67 (2H, s, 2′-H and 3′-H), 5.80 (1′-H, d, J = 1.2 Hz, H-2).

This material (150 mg, 0.5 mmol) was coupled to the protected tyrosinol as described in the preparation of **11** to give **13** as a white powder (11 mg, 4%). υ_{max} (KBr) 1684 cm^{-1}; λ_{max} (H_2O) 274 nm (ε_m 1,487); δ_H (D_2O) 1.24 (3H, t, J = 7 Hz, ethyl), 2.07 (3H, s, Me), 2.4–2.5 (2H, m, 1″-H_2), 2.8–3.0 (2H, m, 3-H_2), 3.5–4.2 (11H, m), 5.14 (1H, s, 3″-H), 6.8 and 7.2 (4H, ABq, tyrosyl aromatics); m/z (ESI^+) 490 (MH^+).

***N*-Boc-L-(*OZ*)tyrosinol (14).** Benzyloxycarbonyl chloride (2.1 mL, 15 mmol) was added to a mixture of *N*-Boc-L-tyrosinol (4.0 g, 15 mmol), triethylamine (2.1 mL, 15 mmol) and dichloromethane (20 mL) at 0°C. After 1 h at room temperature, the solution was washed with aqueous $NaHCO_3$, dried, evaporated and the resulting residue recrystallised from 1:1 ether:hexane to give **14** as white rhombs (3.3 g, 56%). δ_H ($CDCl_3$) 1.44 (9H, s, *t*Bu), 2.84 (2H, d, $J=7$ Hz, 3-H_2), 3.4–3.7 (2H, m, 1-H_2), 3.0 (1H, br s, 2-H), 4.8 (1H, br d, NH), 5.78 (2H, s, ZCH_2), 7.0–7.5 (9H, m, aromatics).

5′-*O*-(L-Tyrosylsulfamoyl) adenosine (15). A solution of 2′,3′-*O*-isopropylidene-5′-*O*-sulfamoyladenosine[17] (0.772 g, 2.0 mmol) in dry DMF (12 mL) was treated with *O*-benzyl-*N*-Boc-tyrosine *N*-hydroxysuccinimide ester (0.936, 2.0 mmol) followed by DBU, (0.3 mL, 2.0 mmol), and the mixture stirred at room temperature for 3 h. The solvent was evaporated and the residue dissolved in ethyl acetate and washed with saturated $NaHCO_3$, 5% $KHSO_4$ and brine, dried (Na_2SO_4) and evaporated to an oil. This was chromatographed on Kieselgel 60 eluting with 10% methanol in dichloromethane to afford the protected product (1.13 g, 76%).

This material was dissolved in 98% formic acid (50 mL). After stirring for 2.5 h at room temperature, the solvent was evaporated and the residue azeotroped with toluene, followed by chromatography on Kieselgel 60 eluting with 10–20% methanol in dichloromethane to give the product as a white foam (432 mg, 47%). This material (175 mg, 0.29 mmol) was dissolved in 1,4-dioxan (5 mL), water (5 mL) and hydrogenated at room temperature and pressure for 5 h over 10% Pd/C (50 mg). The catalyst was removed by filtration, the filtrate concentrated and applied to a column of HP20SS, eluting with 6% THF/water. Product-containing fractions were combined and freeze-dried to give the title compound **15** as a white solid (60 mg, 40%); υ_{max} (KBr) 3353, 1644, 1613 and 1516 cm^{-1}; λ_{max} (H_2O) 260 nm (ε_m 12,134), δ_H (d_6-DMSO) 2.81 (1H, dd, $J=8.0$, 14.3 Hz, Ar CH_2), 3.04 (1H, dd, $J=4.8$, 14.3 Hz, CH_2 Ar), 3.55 (1H, dd, $J=5.2$, 8.4 Hz), 4.06–4.19 (4H, m, 3′, 4′ and 5′H), 4.60–4.62 (1H, m, 2′-H), 5.50 (1H, br s, 2′-OH), 5.93 (1H, d, $J=7.8$ Hz, 1′-H), 7.05 and 6.68 (2×d, $J=8.4$ Hz, Ar-H), 7.23 (2H, br s, NH_2), 8.15 (1H, s), 8.41 (1H, s), 9.21 (1H, br s, OH). *m/z* (ESI) 510 (MH^+, 100%). (ESI-ve) 502 ($[M-H]^-$, 2%), 616 ($[M.TFA-H]^-$, 20%).

5′-Amino-5′-deoxy-2′,3′-*O*-isopropylidene-N^6-benzoyladenosine (18). To a solution containing 2′,3′-*O*-isopropylidene-N^6-benzoyladenosine (1.0 g, 2.5 mmol), triphenylphosphine (1.3 g, 5.0 mmol), sodium azide (1.7 g, 25.0 mmol), and DMF (20 mL) was added carbon tetrabromide (1.6 g, 5.0 mmol). After 2 h at room temperature, ethyl acetate was added and the solution washed with water, dried, evaporated and chromatographed using methanol–dichloromethane mixtures to give the azide as a yellow oil (0.9 g, 80%). δ_H ($CDCl_3$) 1.41 and 1.68 (6H, 2s, CMe_2), 3.60 (2H, d, $J=6$ Hz, 5′-H_2), 4.4, 5.1, 5.4 and 6.2 (4H, 4m, 1′-H, 2′-H, 3′-H and 4′-H), 7.6 and 8.0 (5H, 2m, benzoyl aromatics), 8.33 and 8.82 (2H, 2s, adenine aromatics). The azide was dissolved in ethanol (10 mL) and hydrogenated over 10% palladium on carbon at atmospheric pressure for 3 h. Filtration, evaporation and chromatography using methanol–dichloromethane mixtures gave the amine (**18**) as a colourless oil (0.4 g, 51%). δ_H ($CDCl_3$) 1.30 and 1.58 (6H, 2s, CMe_2), 3.55 (2H, m, 5′-H_2), 4.4, 5.2, 5.4 and 6.1 (4H, 4m, 1′-H, 2′-H, 3′-H and 4′-H), 7.5 and 8.0 (5H, 2m, benzoyl aromatics), 8.35 and 8.82 (2H, 2s, adenine aromatics); *m/z* (DCI) 411 (MH^+).

5′-Aminosulfamoyl-5′-deoxy-2,3-*O*-isopropylidene-N^6-benzoyladenosine (19). A mixture of **18** (110 mg, 0.25 mmol), sulfamoyl chloride (45 mg, 0.38 mmol), triethylamine (0.04 mL, 0.30 mmol) and dichloromethane (2 mL) was stirred at room temperature for 2 h and directly chromatographed using methanol–dichloromethane mixtures to give the sulfamide **19** (80 mg, 65%). δ_H ($CDCl_3$) 1.40 and 1. 62 (6H, 2s, CMe_2), 3.3 (2H, m, 5-H_2), 4.4, 5.2, 5.5, and 6.4 (4H, 4m, 1′-H, 2′-H, 3′-H and 4′-H), 7.5 and 8.0 (5H, 2m, benzoyl aromatics), 8.54 and 8.72 (2H, 2s, adenine aromatics).

***N*-(L-Tyrosyl)-*N*′-(5′-deoxy-5′-adenosinyl)-sulfamide (17).** A mixture of **19** (500 mg, 1 mmol), BocTyr(ONSu) (380 mg, 1 mmol), DBU (0.15 mL, 1 mmol) and DMSO (10 mL) was stirred at room temperature for 2 h then diluted with ethyl acetate. This was washed with water, dried and evaporated, and the resulting residue was chromatographed using methanol–dichloromethane mixtures to give the acylated sulfamide (540 mg, 74%). δ_H ($CDCl_3$) 1.38 (9H, s, *t*Bu), 1.41 and 1.58 (6H, 2s, CMe_2), 2.93 (2H, d, $J=7$ Hz, 3-H_2), 3.3–3.5 (2H, m, 5′-H_2), 3.9 (1H, m, 2-H), 4.5, 4.9, 5.3 and 6.4 (4H, 4m, 1′-H, 2′-H, 3′-H, and 4′-H), 6.6 and 6.9 (4H, ABq, tyrosyl aromatics), 7.5 and 8.0 (5H, 2m, benzoyl aromatics), 7.93 and 8.82 (2H, 2s, adenine). This material (0.54 g, 0.75 mmol), was dissolved in a mixture of *n*-butylamine (3 mL) and methanol (3 mL) and the solution stirred at room temperature for 1 h and then evaporated. The resulting residue was dissolved in a mixture of trifluoroacetic acid (7 mL) and water (5 mL) and the solution stirred for 1 h at room temperature, followed by evaporation and chromatography using HP20SS eluting with acetone–water mixtures to give the desired compound **17** as its trifluoroacetate salt after freeze-drying (110 mg, 27%). υ_{max} (KBr) 1676 cm^{-1}; λ_{max} (H_2O) 261 nm (ε_m 12,328); δ_H (D_2O) 2.9–3.1 (2H, m, 3-H_2), 3.4 and 3.7 (2H, 2m, 5′-H_2) 3.9, 4.1, 4.5 and 5.9 (4H, 4m, 1′-H, 2′-H, 3′-H, and 4′-H), 4.1 (1H, m, 2-H), 6.6 and 7.0 (4H, ABq, tyrosyl aromatics), 8.15 and 8.32 (2H, 2s, adenine aromatics); *m/z* (DCI) 526 (MNH_4^+).

2(*S*)-Amino-3-(4-hydroxyphenyl)propyl 1-(adenin-9-yl)-(*E*)-5,6-dideoxy-β-D-ribohept-5-enofuranuronate hydrochloride (22). Compound **14** (802 mg, 2.0 mmol) was dissolved in dry dichloromethane (5 mL) and treated with *N,N*-dimethylaniline (0.254 mL, 2.0 mmol) followed by bromoacetyl bromide (0.18 mL, 2.0 mmol), and the resultant solution stirred at room temperature for 1 h. The solution was diluted with dichloromethane (20 mL) and washed with saturated $NaHCO_3$, 2 M HCl, water and brine, dried ($MgSO_4$) and evaporated. The product was purified by chromatography on Kieselgel 60 to

afford the bromoacetyl ester as a white solid (0.57 g, 57%). υ_{max} (CH_2Cl_2) 3435, 1760, 1712 and 1501 cm^{-1}; δ_H ($CDCl_3$) 1.41 (9H, s, *t*BOC), 2.82–2.90 (2H, m, $PhCH_2$), 3.87 (2H, s, CH_2Br), 4.10–4.19 (3H, m, CH_2, Hα to NH), 4.65 (1H, br s, NH), 5.27 (2H, s, CH_2Ar), 7.05–7.45 (9H, m, Ar-H); *m/z* (NH_3DCI) 539 (MNH_4^+, 5%), 192 (100). This was dissolved in 1,4-dioxan and heated to 50°C with triphenylphosphine (288 mg, 1.1 mmol) for 8 h. The mixture was cooled, evaporated and azeotroped with toluene to give the crude phosphonium bromide. This was dissolved in chloroform (10 mL) and stirred vigorously with saturated $NaHCO_3$ (10 mL) for 5 min the layers were separated and the process repeated twice. The organic phases were combined, dried ($MgSO_4$) and evaporated to give the phosphorane (**21**) as a white foam, υ_{max} (CH_2Cl_2) 3441, 1759, 1702, 1616 and 1506 cm^{-1}.

2′-3′-*O*-Isopropylidene-N^6-benzoyl adenosine (206 mg, 0.5 mmol) was dissolved in toluene (3 mL) and dry DMSO (1.5 mL) and treated with 1-ethyl-3(3-dimethylaminopropyl)carbodiimide hydrochloride (287 mg, 1.5 mmol), pyridine (0.141 mL, 1.75 mmol) and TFA (0.019 mL, 0.25 mmol) at room temperature under argon. After 18 h, the crude aldehyde was treated with the phosphorane (**21**) (352 mg, 0.5 mmol). After stirring for 1 h the mixture was partitioned between ethyl acetate and water, the organic layer washed with 2 M HCl (×2), saturated $NaHCO_3$, water and brine, dried ($MgSO_4$) and evaporated. The crude product was chromatographed on Kieselgel 60 eluting with 50–100% ethyl acetate/hexane to afford the protected derivative as a white foam (0.217 g, 52%); υ_{max} (CH_2Cl_2) 3431, 1761, 1713 and 1610 cm^{-1}; δ_H (D_2O) (1H, d, *m/z* (ESI) 835 (MH^+, 100%).

The isopropylidine and BOC groups were removed on treatment with 40% TFA/water as described for **2**, to afford the deprotected product (140 mg, 80%) after chromatography. This was dissolved in methanol (2 mL) and treated with *t*-butylamine (0.5 mL). After stirring at room temperature for 1 h, the solvent was evaporated and the residue dissolved in 2M HCl (1 mL). Saturated $NaHCO_3$ was added to adjust the pH to 3.0 and the solution applied to a column of HP20SS, eluting with 0–20% THF/water. Product-containing fractions were combined and freeze-dried to afford the title compound **22** as a white solid (27 mg, 34%); υ_{max} (KBr) 3340, 2925, 1645 and 1515 cm^{-1}; λ_{max} (EtOH) 259 nm (ε_m 15,823), δ_H (CD_3OD) 3.47 (1H, d, $J = 6.5$ Hz, CH_2Ar), 4.11 (2H, d, CH_2O), 4.66–4.78 (1H, m), 5.01 (1H, t, $J = 5.3$ Hz, 3′-H), 5.22–5.28 (1H, m, 4′-H), 5.40–5.44 (1H, m, 2′-H), 6.71 (1H, d, $J = 4.5$ Hz, 1′-H), 6.86 (1H, d, $J = 15.3$ Hz, = H), 7.37 and 7.71 (4H, ABq, $J = 8.3$ Hz, Ar-H), 7.52 (1H, dd, $J = 5.5$, 15.4 Hz). *m/z* (NH_3 + DCI) 457 (MH^+, 30%).

Biochemistry

Tyrosyl tRNA synthetase (YRS) inhibition assays. Pure recombinant *S. aureus* YRS was purified to near homogeneity (~98% as judged by SDS–PAGE) using standard purification procedures. A crude preparation of *B. stearothermophilus* YRS was obtained following a one step purification on a Q Sepharose column. Recombinant YRS activity was measured by the PPi/ATP exchange reaction[23,24] and the aminoacylation activity of crude *Bacillus* YRS was assayed using modifications to a previously described method.[22]

Aminoacylation reaction. The assays were performed at 37°C in a mixture containing 100 mM Tris/Cl pH 7.9, 50 mM KCl, 16 mM $MgCl_2$, 5 mM ATP, 3 mM DTT, 4 mg/mL *E. coli* MRE 600 tRNA (Boehringer Mannheim) and 20 μM/10 μM L-Tyrosine (4 μM [U-^{14}C] L Tyr (Amersham, specific activity: 16.4 GBq/mmol), 6 μM cold L-Tyr). The concentration of inhibitor which results in 50% inhibition (IC_{50}) of YRS activity was determined by preincubating enzyme with a range of inhibitor concentrations for 10 min at room temperature followed by the addition of pre-warmed mix for 5 min at 37°C. The reaction was terminated by adding aliquots of the reaction mix into ice-cold 7% TCA and harvesting onto 0.45 μm hydrophilic Durapore filters (Millipore Multiscreen 96-well plates) and counted by liquid scintillation. The rate of reaction in the experiments were linear with respect to protein and time with less than 50% tRNA acylation. The data was fitted by a least squares procedure using GRAFIT.[25]

PPi/ATP exchange reaction. Pyrophosphate/ATP exchange was monitored in the reverse direction at 37°C in 2 mM [^{32}P]PP_i (specific activity = ~5×10^4 cpm $nmol^{-1}$), 1 mM L-Tyr, 5 mM ATP, 100 mM Tris/Cl pH 7.9, 50 mM KCl, 12 mM $MgCl_2$ and 2 mM DTT. Reactions were quenched after 5 min using 0.4 M pyrophosphate in 7% perchloric acid. The reaction mixture was harvested by adsorption onto activated charcoal which was subsequently collected on Millipore Multiscreen 96-well plates. Following desorption of [^{32}P]ATP from the charcoal using ethanolic ammonia, the concentration of [^{32}P]ATP was determined by liquid scintillation counting. Inhibition assays were carried out as described for the aminoacylation reaction.

Modelling

The tyrosinyl adenylate ligand was removed from the *B. stearothermophilus* tyrosyl tRNA synthetase crystal structure and the enzyme was prepared by adding hydrogens using the CHARMm force field.[9] Tyrosinyl adenylate was then minimised in the active site, with explicit solvation and relaxation of both the protein and the ligand. The novel ligands were built from the tyrosinyl adenylate structure and were minimised to convergence in the *B. stearothermophilus* active site with explicit salvation and relaxation of both the protein and the ligand. Only conformations similar to those of the bound tyrosinyl adenylate were considered. The resulting complexes were analysed in terms of protein–ligand interactions, the presence of any deformation within the protein active site, and the strain energy of the ligand.

In the case of the phosphate replacements, some large scale conformational sampling of the ligands was carried out within the constraints of the active site. This

involved Monte Carlo conformational sampling in the rigid active site in order to generate 100 structures. Torsion increments of 30° were used, the temperature was set to 5000 K and 50 steps of steepest descent minimisation were performed in each case. The 20 structures of lowest energy were then minimised to convergence within the active site, using the adopted-basis Newton–Raphson algorithm. No constraints were imposed on either the ligand or a 20 Å sphere of the protein around the active site. The monomeric unit of tyrosyl tRNA synthetase was used throughout and explicit solvation was employed. The sulfamate and sulfamide containing compounds were modelled as zwitterions as this is the form seen in the X-ray crystal structure of the analogous alanyl sulfamoyl adenosine.[7]

Sequence alignments were performed using ClustalW.[26] Homology modelling was carried out within Quanta,[9] with use of the rotamer libraries to optimise side chain placement. The model was refined using the CHARMm force field[9] with a constant dielectric and explicit solvation. Tyrosinyl adenylate was docked into the active site, both in its crystallographically observed conformation and after allowing Monte Carlo sampling of the ligand within the enzyme active site. The results from the two approaches were in good agreement.

Acknowledgements

The authors thank Mary McVey and Paul Carter for protein purification.

References and Notes

1. Walker, G.; Brown, P.; Forrest, A. K.; O'Hanlon, P.; Pons, J. E. In *Recent Advances in the Chemistry of Anti-infective Agents*; Royal Society of Chemistry, London, 1993; p. 106.
2. Brick, P.; Bhat, T. N.; Blow, D. M. *J. Mol. Biol.* **1989**, *208*, 83.
3. Fersht, A. R.; Shindler, J. S.; Tsui, W.-C. *Biochemistry* **1980**, *19*, 24.
4. Sandrin, E.; Boissonas, R. A. *Helv. Chim. Acta* **1966**, *24*, 273.
5. Desjardins, M.; Garneau, S.; Desgagnes, J.; Lacoste, L.; Yang, F.; Lapointe, J.; Chenevert, R. *Bioorg. Chem.* **1998**, *26*, 1–13.
6. Belrhali, H.; Yaremchuk, A. *Science* **1994**, *263*, 1423.
7. Ueda, H.; Shoku, Y. *Biochim. Biophys. Acta* **1991**, *180*, 126.
8. Heacock, D.; Forsyth, C. J.; Shiba, K.; Musier-Forsyth, K. *Bioorg. Chem.* **1996**, *24*, 273.
9. Molecular Simulations Inc.; 16, New England Executive Park, Burlington, MA, 01803-S297.
10. Eriani, G.; Delarue, M.; Poch, O.; Gangloff, J.; Moras, D. *Nature* **1990**, *347*, 203.
11. Allen, F. H.; Bellard, S.; Brice, M. D.; Cartwright, B. A.; Doubleday, A.; Higgs, H.; Hummelink, T; Hummelink-Peters, B. G.; Kennard, O. et al. *Acta Crystallogr., Sect. B* **1979**, *B35*, 2331.
12. Hodgson, J. E.; Lawlor, E. J. Eur. Pat. Appl., EP 785258 Al.
13. Available from http://www.concentric.net/~ketchup/genedoc/shtml.
14. Wilkinson, A. J.; Fersht, A. R.; Blow, D. M.; Carter, P.; Winter, G. *Nature* **1984**, *307*, 187.
15. Cassio, D.; Lemoine, F.; Waller, J.-P.; Sandrin, E.; Boissonas, R. A. *Biochemistry* **1967**, *6*, 827.
16. Chladek, S.; Smrt, J. *Coll. Czech. Chem. Commun.* **1964**, *29*, 214.
17. Castro-Pichel, J. et al. *Tetrahedron* **1987**, *43*, 383.
18. Aslani-Shotorbani, G. et al. *Carbohydrate Research* **1985**, *136*, 37.
19. Ohrui, H. et al. *Agr. Biol. Chem.* **1972**, *36*, 1651.
20. Kasher, B. et al. *Synthesis* **1990**, 1031.
21. Mann, J. et al. *J. Chem. Soc. Perkin Trans. 1* **1988**, 433.
22. Calender, R.; Berg, P. *Biochemistry* **1966**, *5*, 168.
23. Pope, A. J.; Lapointe, J.; Mensah, L.; Benson, N.; Brown, M. J; Moore, K. J. *J. Biol. Chem.* **1998**, *273*, 31680.
24. Pope, A. J.; Moore, K. J.; McVey, M.; Mensah, L.; Benson, N.; Osborne, N.; Broom, N.; Brown, M. J. *J. Biol. Chem.* **1998**, *273*, 31691.
25. Leatherbarrow, R. J. *Grafit* Version 3.0, Erithacus Software Ltd, Staines, UK.
26. Thompson, J. D.; Higgins, D. G.; Gibron, T. J. *Nucleic Acids Research* **1994**, *22*, 4673.
27. Arnez, J. G.; Moras, D. *Trends Biochem. Sci.* **1997**, *22*, 189.